2024 IEEE Aerospace Conference, 02-09 March 2024, Big Sky, MT, USA
DOI: 10.1109/AERO58975.2024.10521441

Conceptual Design Study Based on Defined Parameters for Next-Generation Martian Rotorcrafts

Vishal Youhanna
School of Aerospace, Transport and Manufacturing.
Cranfield University
Cranfield, UK
Vishal.Youhanna@cranfield.ac.uk

Leonard Felicetti
School of Aerospace, Transport and Manufacturing.
Cranfield University
Cranfield, UK
Leonard.Felicetti@cranfield.ac.uk

Dmitry Ignatyev
School of Aerospace, Transport and Manufacturing.
Cranfield University
Cranfield, UK
D.Ignatyev@cranfield.ac.uk

Abstract— **The remarkable achievement of NASA's Ingenuity Helicopter has opened exciting possibilities for the future exploration of Mars, suggesting that aerobots will play a crucial role alongside rovers and landers. However, Ingenuity's capabilities are limited by its small and relatively basic design. This limitation is primarily evident in its restricted long-range endurance and limited capacity for scientific payloads. To address these shortcomings and advance the field of Martian drone technology, this paper introduces a practical approach to optimising the Martian rotorcraft concepts within the set parameters. The primary objective of these concepts is to enhance performance, endurance, and payload capacity to meet more demanding requirements for future Martian aerobot missions. The paper addresses an essential phase in the design process—an initial sizing of rotary electric vertical takeoff and landing (eVTOL) configurations. This phase is informed by a comprehensive parametric analysis, which considers various factors affecting the performance of drones during hover (stationary flight), vertical climb (ascending flight), and forward flight. The analysis is based on the principles of simplified rotorcraft momentum theory, a foundational concept in rotorcraft engineering. These Martian drone concepts are tailored to address the more challenging mission requirements that future Martian exploration missions are likely to demand. These requirements may include extended flight durations, increased payload capacity to accommodate scientific instruments, and the ability to cover larger areas on the Martian surface. Importantly, the designs are constrained by the maximum size of the spacecraft aeroshell, ensuring that they can be safely transported to Mars within the confines of the protective aeroshell. Among the various configurations considered in this study, a tandem rotorcraft configuration emerged as the most efficient option. This configuration is expected to attain a balance between performance, endurance, and payload capacity, making it a promising choice for future Martian aerobot missions. In contrast, the analysis revealed that a conventional single main rotor configuration within the defined parameters performed poorly in meeting the requirements of the mission.**

TABLE OF CONTENTS

1. INTRODUCTION

Interest in Mars exploration is increasing, and there is a need to design specialised flying robots called aerobots to ensure future missions are sustainable in the thin atmosphere of Mars. Up until a few years ago, Mars was mainly explored using orbiters, landers, and rovers. However, the concept of using unmanned flying vehicles has gained traction due to their advantages over traditional surface rovers, such as speed, range, obstacle avoidance, and broader visibility [1]. Historically, planetary exploration research focused on lighter-than-air airships or fixed-wing planes due to the technical complexity of rotating-wing aerobots. Yet, recent advancements in terrestrial drone technology have sparked more interest in this field. This technological progress led to the creation, launch, and successful landing of the first operational aerobot on Mars in 2021.

Mars' distinct features pose unique challenges for rotorcraft design, predominantly due to its atmospheric conditions. Despite Mars' gravity being only around 38% of Earth's, the average atmospheric density on Mars is roughly 100 times lower than Earth's [2]. Consequently, rotor operations on Mars involve extremely low Reynolds numbers, even lower than 5000 for small-scale helicopters. However, the Mach number is considerably higher ($M>0.4$) due to the requirement for increased tip speed (attributed to lower density), coupled with the fact that Mars' speed of sound is approximately 72% of Earth's. This combination of low Reynolds numbers and high Mach numbers presents considerable design constraints for rotorcraft [3]. An essential challenge for sustaining the flight of a Martian drone involves minimizing or rejecting heat generated by the propulsion system while generating the necessary lifting thrust. This task is exceedingly challenging given the low Reynolds numbers involved. In addition, these challenges are further complicated by the size limitation of the aeroshell (maximum diameter of 4.5 meters) used for transporting the aerobot to Mars [4]. All of these complexities have cast doubt on the feasibility of flying rotating-wing aerobots on Mars in the past, until the successful deployment of the first Martian

helicopter.

The feasibility of unmanned rotorcraft flight on Mars has been conclusively demonstrated by NASA's Ingenuity Mars Helicopter. This vehicle successfully landed on Mars in February 2021 and, by the end of 2023, has completed 70 short autonomous pre-commanded flights. It has flown for a total of about 128 minutes, covering 17 km, achieving altitudes as high as 24 m, and achieving a ground speed of up to 10 m/s [5]. These flight tests have enabled Ingenuity to transition from the Technology Demonstration phase to the Operations Demonstration phase, showcasing the potential collaboration between future rovers and aerial surveyors [5]. The experience gained from the design and operation of the Mars Helicopter can be leveraged to create more advanced aerobots for Mars exploration. While the Ingenuity Helicopter has demonstrated the capabilities of unmanned aerial vehicles on Mars, its design limitations, such as its small size and basic configuration, restrict its endurance, range, and payload capacity. These limitations hinder its ability to conduct comprehensive scientific exploration missions requiring long-distance flights, greater scientific payloads, advanced communication systems, or powerful propulsion systems for high-altitude flights.

As a response, we aim to enhance the design of such aerobots by proposing a new set of more ambitious requirements for Martian aerobot missions. This will lead to the development of a new rotorcraft design. We are mindful of the practicality of the design, ensuring it fits within the constraints of a maximum aeroshell diameter of 4.5 meters, assuming that launch and re-entry technologies will remain relatively stable over the coming decades. Our proposed mission location is the South-West (SW) Melas Basin of Melas Chasma, situated at approximately 9.81 degrees south latitude and 76.47 degrees west longitude. This location is within the Valles Marineris canyon system on Mars. While this site has previously been of interest to scientists, its rugged terrain has posed challenges. However, advancements in navigational planetary landing technology, combined with the obstacle avoidance capabilities of aerobots through flying, make this site a promising candidate for in-situ exploration [3]. An aerobot deployed in this region could create high-resolution aerial maps and identify potential locations for experimental sample collection for future rover missions. The primary objective of the mission is to capture high-quality images of the surveyed areas and effectively transmit this visual data to a rover (belonging to the same mission) or a ground control station on Earth.

One conceivable method of enhancing the capabilities of Ingenuity Helicopter is by introducing fixed wings to its design. Various proposals for Mars exploration have included fixed-wing aircraft with vertical takeoff and landing (VTOL) capabilities, featuring both rigid and foldable body configurations [6]-[15]. Integrating wings into the existing design could extend the endurance and payload capacity of the helicopter. To achieve this, one approach is to utilise the same rotor blades as the Ingenuity Helicopter or optimise the airfoil based on the advanced Mars Science Helicopter [15]. This could result in the design of a VTOL foldable fixed-winged Mars drone, providing additional space for carrying larger scientific payloads and accommodating more solar panels. However, a larger aerobot would either need separate transportation to Mars or would have to be packaged with a smaller rover or lander, given the existing constraints of the aeroshell size. Incorporating a folding mechanism within the aeroshell might be necessary. Thus, a comprehensive parametric study of rotorcraft configurations is required to definitively determine whether the integration of wings into Martian rotorcraft is beneficial overall, and if so, the optimal configurations to pursue.

In this paper, for the Martian environment, the relationship between rotor disk area and power required for hover, vertical climb, and forward flight of various rotorcraft configurations is analysed, based on the parameters defined by the Mars exploration mission specifications, using simplified momentum theory. Consequently, the initial sizing of these battery-electric rotorcrafts is estimated.

2. METHODOLOGY FOR POWER REQUIREMENT ANALYSIS OF ROTORCRAFTS

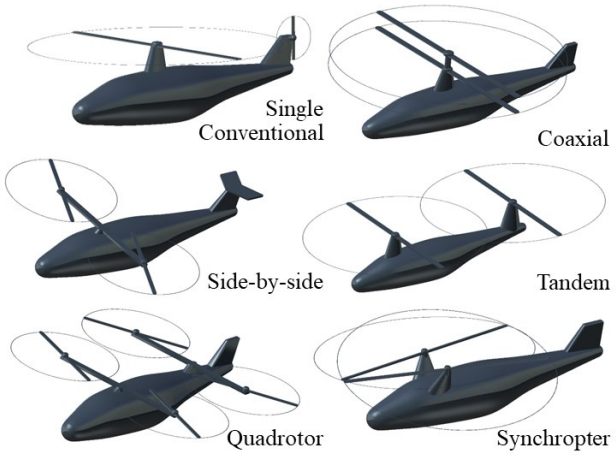

Fig. 1 Rotorcraft Configurations Illustrations

A conventional helicopter features a single main rotor positioned on top and a tail rotor at the rear. The main rotor provides lift and thrust, while the tail rotor counteracts the torque produced by the spinning of the main rotor. In a coaxial helicopter, two rotors are stacked on top of each other on the same axis. They rotate in opposite directions, eliminating the need for a tail rotor. This design enhances stability and maneuverability. Whereas tandem rotorcraft has two main rotors, one positioned in front of the other on the same fuselage. This configuration offers excellent lift capacity and load-carrying capabilities. Side-by-side rotorcraft have multiple rotors positioned next to each other, either on the same or separate planes. They include configurations like tiltrotors and tiltwings, which provide

versatility in both hovering and forward flight. A synchropter is a subtype of side-by-side rotorcraft with two counter-rotating rotors set at outward-tilting angles. They share a single gearbox to ensure the rotor blades do not collide. A quadcopter is a type of multicopter with four rotors arranged in a square configuration. These are known for their simplicity, stability, and ease of control. Therefore, these are widely used in drones and UAVs.

Conventional Rotorcraft (single on Fig. 1)

The key factor for the successful flight of a reusable Martian aerobot on Mars is its ability to perform vertical takeoff and landing (VTOL) since there are no runways available. This capability is entirely dependent on the rotary propulsion system of the rotorcraft. The momentum theory is used to estimate the power consumption of the rotor during hover, vertical climb, and forward flight. In this theory, it is assumed that the rotor blades, while spinning, act as an actuator disk with negligible thickness and a specific disk area (S). Several other assumptions are made, including the presence of uniform airflow throughout the rotor disc and an instantaneous transfer of energy to the airflow. Additionally, certain factors like airfoil profile drag losses, tip losses, and residual rotational velocities are disregarded. To account for these losses, a parameter known as the figure of merit (M) is introduced. This figure of merit (M) represents the ratio of ideal power to actual power ($M=P_{ideal}/P_{actual}$) and serves as a measure of rotor efficiency. Equation (1) calculates the power required for the vertical (vert) climb or hover (when the climb velocity is zero), specifically for a conventional helicopter [16]. The total power calculated also includes the power needed for the tail rotor. The ratio of power required by the tail rotor to that required by the main rotor ($P_{tail\ rotor}/P_{main\ rotor}$) typically falls within the range of 0.14 to 0.22, as tail rotors typically have a diameter of about 15-20% of the main rotor's diameter [16].

$$P_{(\text{Vert Climb or Hover})} = \left[\left(\frac{fW}{M}\sqrt{\frac{fW/S}{2\rho}}\right) + \frac{WV_{Climb}}{2}\right]\left[\frac{(1+P_{\text{tail rotor}}/P_{\text{main rotor}})}{\eta_{mechanical}}\right] \quad (1)$$

Where:
P = power required; W = helicopter weight; S = rotor disk area; M = measure of merit; V_{climb} is vertical climb speed (= 0 for hover); f is the adjustment for downwash on the fuselage (typically f = 1 .03); ρ = Martian air density; $\eta_{mechanical}$ is mechanical losses adjustment due to driving of tail rotor (typically $\eta_{mechanical} = 0.97$)

In forward flight, the rotor acts like a circular wing. The aspect ratio of such a wing is $4/\pi$, with an equivalent Oswald efficiency factor of 0.5 to 0.8 based on empirical data. Oswald efficiency factor of the wing at a given lift coefficient is defined as the ratio of the wing's induced drag coefficient and induced drag coefficient of the equal aspect ratio elliptic wing at that same lift coefficient. Parasitic drag can be given in terms of drag area (D/q), where q is the dynamic pressure. Equation (2) comprising these factors, produces required power estimates for forward climb or level flights [16]. $Wsin(\gamma)$ in the equation is the climb component which depends on the climb path angle γ (0 for leveled flight). The rotor produces forward flight propulsion acting as a propeller, along with maintaining the lift. Therefore, the propellor efficiency factor η_p is added into the calculation to give a reasonable estimate of the rotor in forward thrust.

$$P_{(\text{Fwd}_{\text{climb}}\text{ or }\text{Fwd}_{\text{level}})} = \left[\frac{V}{\eta_p}\left\{q(D/q) + \frac{W^2}{4eqS} + Wsin(\gamma)\right\}\right]\left[\frac{(1+P_{\text{tail rotor}}/P_{\text{main rotor}})}{\eta_{mechanical}}\right] \quad (2)$$

Where:
V = forward flight speed; γ = climb path angle (=0 when levelled); q = dynamic pressure; e = equivalent Oswald efficiency factor (0.5 to 0.8); (D/q) = component drag area; η_p = propeller efficiency (0.6 to 0.85)

Coaxial Rotorcraft (Fig. 1)

In a conventional helicopter setup, the primary role of the tail rotor is to counteract the torque generated by the spinning of the main rotor. It achieves this by producing an equal but opposite thrust force, which provides a balance in torque. However, an alternative approach to resolving the torque issue is to replace the tail rotor with another rotor of equal size but rotating in the opposite direction. This second rotor generates thrust in the same direction as the main rotor, offering the advantage of additional lift. One configuration that employs this concept is the coaxial rotorcraft, where two rotors are mounted on the same shaft within a more complex hub arrangement. At first glance, it might seem that this configuration would double the lift force. However, due to the proximity of the two rotors, some lift is lost due to interference caused by the airflow wake. Theoretically, when the two rotors perfectly overlap, which is a 100 percent overlapping case with a zero vertical gap, the overlapping interference factor (K_{ov}) increases power consumption by approximately √2 or about a 41% increase compared to two isolated rotors that are not influenced by the wake of the upper rotor [17]. When there is no vertical spacing between the rotors in a coaxial setting, it is termed an equivalent single rotor. This equivalent single rotor is equated to a system of smaller twin rotors with the same total thrust and total projected area (disk loading) because they share the same rotor solidity, which is the ratio of the total blade area to the total disk area [18].

In practice, coaxial rotor systems have a mechanical separation between the two rotors, and as this vertical separation increases, the wake of the upper rotor affects a

smaller area of the lower rotor. Therefore, the overlapping interference factor (K_{ov}) decreases. For instance, with a large separation (LS), typically around 10% of the rotor diameter, the K_{ov} becomes 1.281 when assuming uniform disk loading [17][18]. As a result, Eq.(1), to calculate vertical climb and hover power for a coaxial rotor system with two equal-sized rotors equally sharing the total rotorcraft weight (thrust), is adjusted by multiplying it by the overlapping interference factor (K_{ov}) to form Eq. (3). Similarly, Eq. (2) for forward flight of conventional helicopter is adjusted to form Eq. (4) for a coaxial helicopter [17]. In this configuration, there is no tail rotor, but instead, a second rotor is used. Consequently, the ratio of power required by the two equal-sized rotors ($P_{second\ rotor}/P_{main\ rotor}$) becomes 1.

$$P_{(\text{Vert Climb or Hover})} = \left[\left(\frac{fW}{(2\sqrt{2})M}\sqrt{\frac{fW/S}{2\rho}}\right) + \frac{WV_{Climb}}{4}\right]\left[\frac{2}{\eta_{mechanical}}\right][K_{ov}] \quad (3)$$

$$P_{(\text{Fwd}_{climb}\ \text{or}\ \text{Fwd}_{level})} = \left[\frac{V}{\eta_p}\left\{q(D/q) + \frac{W^2}{16eqS} + \frac{Wsin(\gamma)}{2}\right\}\right]\left[\frac{2}{\eta_{mechanical}}\right][K_{ov}] \quad (4)$$

Isolated Rotors (e.g., side-by-side in Fig 1)

The K_{ov} factor, denoting the extent of overlapping interference between two equal-sized rotors, undergoes a transition from $\sqrt{2}$ to 1 when the shared area between them in the same plane changes from complete to none. In the latter scenario, these rotors essentially function as isolated units. However, there might still be a minor degree of either advantageous or disadvantageous interference in cases where there is vertical separation between the rotors without any overlap, which can be safely disregarded in preliminary study scenarios [17][18]. In situations involving configurations of multiple rotors with no overlap, Equations (1) and (2) can be adapted to account for a multirotor system comprising 'N' equal-sized rotors. In such an arrangement, the total thrust required for the rotorcraft is evenly distributed among all the rotors, expressed in Equations (5) and (6). However, in forward flights, the configurations that have rotors aligning in front of the other rotors, there is an added downwash factor generated by the front rotor upon the rear rotor. This downwash would need to be accounted for and be factored into the rear rotor/s to estimate the actual power required, as shown in the following section about the tandem case [17]. Since there is no tail rotor in such a setup, the ratio of power required by the tail rotor to that required by the main rotor ($P_{tail\ rotor}/P_{main\ rotor}$) is replaced by (N – 1) in the equation to account for the number of rotors.

$$P_{(\text{Vert Climb or Hover})} = \left[\left(\frac{fW}{(N\sqrt{N})M}\sqrt{\frac{fW/S}{2\rho}}\right) + \frac{WV_{Climb}}{2N}\right]\left[\frac{N}{\eta_{mechanical}}\right] \quad (5)$$

$$P_{(\text{Fwd}_{climb}\ \text{or}\ \text{Fwd}_{level})} = \left[\frac{V}{\eta_p}\left\{q(D/q) + \frac{W^2}{(N^2)4eqS} + \frac{Wsin(\gamma)}{N}\right\}\right]\left[\frac{N}{\eta_{mechanical}}\right] \quad (6)$$

Tandem Rotorcraft and Side-by-side Rotorcraft (Fig 1)

In a tandem rotorcraft configuration, two equal-sized rotors are aligned longitudinally on the fuselage, with one rotor located in front of the other. Theoretical analysis of this setup is like that of coaxial rotors, as it has overlapping disk area which depends on the horizontal gap between the rotors, with maximum tandem overlap being when the blade tip of one rotor touches the hub centre of the other rotor. Therefore, the preliminary vertical climb or hover power analysis for tandem rotors follows the same formula as that used for coaxial rotors, as described in Eq. (3). However, the calculation of the overlapping interference factor (K_{ov}) in a tandem configuration is influenced by the ratio (d/D), which represents the horizontal distance (d) between the two rotor axes to the rotor diameter (D). When the rotors are in the same plane (i.e., no vertical gap between rotors), K_{ov} can be approximated using Eq. (7) [17].

$$K_{ov} = \left[\sqrt{2} - \frac{\sqrt{2}}{2}\left(\frac{d}{D}\right) + \left(1 - \frac{\sqrt{2}}{2}\right)\left(\frac{d}{D}\right)^2\right] \quad (7)$$

In situations where the rotors are in separate planes, and the lower rotor operates within the contracting wake of the upper rotor, the determination of the overlapping area requires numerical integration to find a solution for K_{ov}. Additionally, there are side-by-side rotor configurations with overlapping rotors that can use a similar approach to estimate the total power required. One such configuration is the synchropter, which features two counter-rotating rotors set at outward-tilting angles and a single gearbox to prevent blade collisions. Another subtype is transverse rotorcraft, including tiltrotors and tiltwings, where smaller rotors are mounted horizontally on the tips of side wings or an extended support frame of the fuselage. These smaller rotors are normally positioned to not overlap and function more like isolated rotors. During a cruise flight, they convert into forward propellers. These various rotorcraft configurations each have their unique characteristics and aerodynamic considerations, and the choice between them depends on specific mission requirements and design objectives [17][18].

However, for forward flight estimation of tandem rotorcraft the rear rotor experiences downwash from the front rotor, which needs to be computed and added to the power loss. For initial theoretical analysis, this downwash (dw) is assumed to be the maximum value of overlapping interference factor (max $K_{ov} = K_{dw}$), which is 1.134 when calculated using Eq. (7) at maximum tandem overlap [17]. So total power (P) required for forward flight is represented by Eq. (8) [17]. For the preliminary analysis, it is assumed that the two equal-sized rotors produce equal amounts of thrust and thus, require equal amounts of power. Hence, this expression is represented in Eq.(9), where the total power of 2 isolated rotors (calculated using Eq. (6)) is halved and then one-half is multiplied by the downwash factor. If there is an overlap between these two rotors, then the K_{ov} is further factored into the expression to estimate the total forward power.

$$P_{(Forward)} = P_{Front\ Rotor} + P_{Rear\ Rotor}(K_{dw}) \quad (8)$$

$$P_{(Forward)} = (1 + K_{dw})\frac{1}{2}P_{2\ Iso}K_{ov} \quad (9)$$

Where:
$P_{2\ Iso}$ is required forward flight power of rotorcraft with 2 isolated rotors; K_{dw} (= 1.134) is the downwash factor; K_{ov} (= 1 when no overlapping) is the overlapping interference factor

3. Methodology for the Initial Sizing of Battery-Electric Aircraft

The overall maximum take-off weight of an aircraft consists of three components: the empty weight, the payload, and the fuel. In the case of fuel-burning aircraft, the weight decreases during flight due to the gradual consumption of fuel across different flight segments, including taxiing, takeoff, ascent, cruising, and descent. This weight reduction affects the performance and drag characteristics of aircraft, so initial sizing estimates involve calculations for each of these flight phases. In contrast, electric aircraft do not experience changes in battery mass during flight. Therefore, there is no need to integrate calculations across various flight segments. Instead, the fuel component of the total aircraft weight is replaced by the weight of the battery (W_b). The required battery mass for each mission segment is determined using Eq. (10), which expresses it as a ratio of the battery mass to the total aircraft mass (m_b/m), known as the Battery Mass Fraction (BMF). Equation (10) considers factors such as the known run-time endurance (E) and the power consumed during different flight segments, including vertical climb, hover, and forward flight for rotorcraft. The total required aircraft BMF is then obtained by summing the BMFs of each mission segment [16]. This approach allows for a comprehensive assessment of the battery mass required for various phases of the aircraft's mission.

$$BMF = \frac{m_b}{m} = \frac{W_b}{W_0} = \frac{EP_{used}}{E_{sb}\eta_{b2s}m} \quad (10)$$

Where:
m_b = battery mass; m = aircraft total mass; W_b = battery weight; W_0 = aircraft total take-off weight; P_{used} = power required (Watt = W); E = known run time (hour = h); E_{s2b} = battery specific energy {W.h/kg}; η_{b2s} = total system efficiency from the battery to the motor output shaft (typically $\eta_{b2s} \sim 0.9$)

Equation (11) is used to determine the total aircraft take-off weight (W_0), by showing that it is equal to the empty weight, the battery weight, and the payload weight. Eq. (11) undergoes modification to formulate Eq. (12) for electric aircraft sizing. This adjustment involves factoring in the total Battery Mass Fraction and the ratio of empty weight (W_e) to total weight [16]. In this context, the payload can take the form of instruments or objects to be delivered, particularly in the case of unmanned aircraft. In contrast, W_e encompasses all components except for the payload or functional batteries, including the propulsion system, aircraft structure, avionics, navigation equipment, and other essential systems.

$$W_0 = W_e + W_b + W_{payload} \quad (11)$$

$$W_0 = \frac{W_{payload}}{1 - BMF_{total} - \frac{W_e}{W_0}} \quad (12)$$

The initial sizing equation provides an initial estimation point, allowing for preliminary estimations based on factors such as the empty weight ratio, payload weight (informed by statistical data), and the calculated required Battery Mass Fraction (BMF). These values can be utilized to determine the total weight. Alternatively, known parameters can be used to deduce unknown variables, such as estimating the total weight and empty weight and then computing the required BMF to assess the aircraft's payload capacity. This sizing procedure can be iterative and may require multiple calculations and adjustments until a reasonable estimate aligns with the desired objectives, facilitating preliminary design investigations.

4. Definition of Parameters for Analysis

Overall Parameters

The key parameter for the initial power sizing analysis of rotorcraft is the air density, which is typically encountered during its flight. Mars' mean surface air density is approximately 0.02 kg/m^3 [19], although it can vary depending on location, altitude relative to sea level, and changes over seasons and time of day. For the primary mission in SW Melas Chasma, which is situated around 2 km below the datum, the Mars Climate Database (Version 5.3) [20] was used to estimate regional air density values at a flight time corresponding to the 11th-hour local solar time [21][3]. This analysis resulted in a mean air density estimate

of 0.016 kg/m3.

Another critical parameter is the constraint imposed by the maximum size of the aerobot. The size of the protective heat shield, known as the aeroshell, which encapsulates the spacecraft carrying the aerobot to Mars, serves as a limiting factor. To design and analyse possible Martian aerobot configurations, the maximum existing aeroshell size with a diameter of 4.5 m and a height of approximately 2.2 m has been defined. For this parametric study, a range of rotor diameters spanning from 0.23 m to the maximum allowed diameter of 4.5 m is analysed, whereas an actual rotor design would include clearance from the internal wall of the aeroshell.

Table 1 Parameters used in the forward flight, vertical climb and hover power analysis of different configurations of rotorcrafts.

Parameter	Values			Unit
Mean Air Density	0.016			kg/m3
Speed of Sound	240.00			m/s
Limit of Max Rotor Blade Tip Speed	0.75			Mach
Mars Speed at Max Rotor Tip Speed	180.00			m/s
Max Forward Flight Speed, V	60.61			m/s
Cruise Flight Endurance, E	11.00			min
Dynamic Pressure at the Max Fwd Speed, q	29.38			Pa
Average Vertical Climb Velocity, V_{climb}	16.00			m/s
Vertical Climb Endurance, E	1.00			min
Aircraft MTOG Mass	20			kg
Aircraft MTOG Weight, W	74.42			N
Rotor Blade Diameter, Blade D	0.23	to	4.5	m
Rotor Disk Area, S	0.04	to	15.9	m2
Battery Specific Energy, E_{s2b}	230.00			W.h/kg
Measure (or figure) of Merit, M	0.7			
Mechanical efficiency factor, $\eta_{mechanical}$	0.97			
Fuselage downwash adjustment, f	1.03			
Helicopter Power ratio ($P_{tail\ rotor}/P_{rotor}$)	0.18			
Coaxial Power ratio ($P_{second\ rotor}/P_{main\ rotor}$)	1			
System efficiency battery to motor (η_{b2s})	0.9			
Propeller Efficicency, η_p	0.8			
Oswald Efficiency, e	0.65			
Parasitic Drag Area, D/q (Front Area x Drag data)	Front Area	Drag Data	D/q	
D/q Fuselage (radius 0.15 m)	7.1E-02	0.09	6.0E-03	m2
D/q Tubular Landing 4 legs (0.002m x 0.03m, each)	2.4E-04	1.01	2.4E-04	m2
D/q Unfaired Single Rotor (0.005m x 0.003m)	1.5E-05	1.20	1.8E-05	m2
Downwash Interference Drag Fuselage	7.1E-02	0.02	1.4E-03	m2
Leakage & Protuberance Drag (15% Total D/q)			1.2E-03	m2

Additionally, specific values have been set for various parameters, including a maximum forward velocity of 60.6 m/s, which is a quarter of the average speed of sound on Mars (240 m/s) [3] and one-third of the maximum permitted rotor tip speed. To ensure that the rotorcraft generates lift on the retreating blade, the advancing blade must move at possibly three times the helicopter's airspeed. However, to prevent the buildup of transonic compression waves, the maximum tip speed of a rotor is limited to around 0.75 Mach [16]. At this forward speed, the aerobot aims to cover 40 km ground distance in 11 mins. The results using such a theoretical method are in good agreement with experimental data when the advance ratio of aircraft is from 0.1 to 0.3 [17]. The advance ratio of rotorcraft is the ratio of its forward flight speed to its rotor tip speed. For vertical take-off, the goal is to ascend to 1 km in 1 minute, resulting in a maximum vertical climb (V_{climb}) velocity of approximately 16 m/s.

For the forward flight analysis, certain perimeters are essential such as the frontal area of the body of aircraft. For all the configurations the same frontal area of the fuselage, landing legs, and an unfaired rotor hub are used. D. Raymer [16] has listed helicopter-specific drag data in terms of drag area (D/q) (per unit frontal area), which can be multiplied by the helicopter's frontal area to get the specific values of the drag area of each component. The total parasitic drag calculated is then fitted into Eq. (2) for the conventional helicopter, whereas forward flight equations for other rotorcrafts are adjusted accordingly. The drag data is not a precise way of calculating parasitic drag but is suitable for the initial sizing of the rotorcraft until the design becomes mature for further preliminary study.

The total mass of the aerobot for the mission is set at 20 kg. The measure of merit, denoted as M, typically falls within the range of 0.6 to 0.8 [16]; so an average value of 0.7 is used. The battery's specific energy E_{s2b}, used for vertical climb Battery Mass Fraction (BMF) calculations, is estimated at 230 Wh/kg, based on a JPL technology forecast [4]. Table 1 provides a summary of the parameters mentioned above, which are employed in the power analysis for different rotorcraft configurations during forward flight, vertical climb, and hover phases.

Tandem Rotors Cases

Tandem rotorcraft can take on various configurations depending on how the rotors are positioned longitudinally on top of the fuselage. For the power consumption analysis, three cases are considered based on the structural extremities of the aeroshell. Assuming the fuselage length matches the size of the maximum aeroshell, which is 4.5 m, the two equal-sized rotors are positioned at equal displacements from the mid-point, resulting in displacements of 2.25 m, 1.125 m, and 0.75 m for Cases 1, 2, and 3, respectively [22]. This arrangement is illustrated in Fig. 2. The maximum rotor diameter is 9 m for Case 1, 4.5 m for Case 2, and 3 m for Case 3. It is worth noting that, in practical design, there would be required clearances for rotor blades from the inner walls of the aeroshell and rotor hubs. However, for this theoretical analysis, such clearances are not considered.

In all cases, when the rotor diameter (D) is equal to or less than half of the maximum diameter (D max), the rotors no longer overlap, and it is assumed that these behave as isolated rotors. When the rotors exhibit isolated behavior, the rotorcraft essentially functions as a multicopter design rather than a tandem rotors configuration. The K_{ov} is 1 when there is no overlapping. However, Eq. (7) would provide a range of values that are initially lower than 1 and then transition to

above, when the rotor size decreases and the gap between the edges of two rotors keeps increasing - this intentionally would need to be corrected to 1.

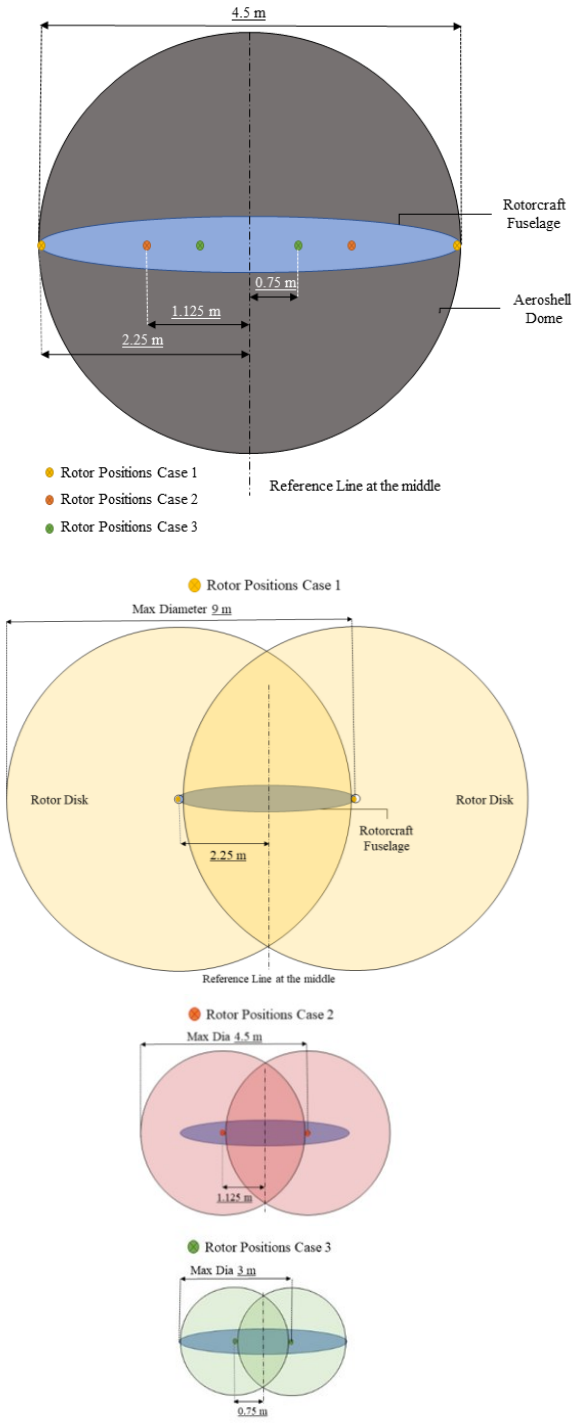

Fig. 2 Schematic illustration of the rotor positioning of tandem rotorcraft Cases 1, 2, and 3. (Not to scale)

Case 1 necessitates an articulated rotor hub system with a folding mechanism to fit within the aeroshell for storage. Case 2 would also require similar folding mechanisms and an articulated rotor hub system if the rotor diameter exceeds 2.25 m. Conversely, Case 3 can employ a rigid rotor hub system without the need for linkages. Table 2 provides a summary of the defined parameters for all three study cases of tandem rotorcraft.

Table 2 Summary of Tandem Rotorcraft Cases

Case No.	Rotor System Type	Folding Mechanism	Maximum Diameter	Rotor Position*	Isolated Rotor behaviour
1	Articulated	Yes	9 m	2.25 m	D ≤ 4.5 m
2	Articulated**	Yes**	4.5 m	1.125 m	D ≤ 2.25 m
3	Rigid	No	3 m	0.75 m	D ≤ 1.5 m

* Rotor hub position from the center of the fuselage

** When rotor D is > 2.25 m

5. RESULTS AND ANALYSIS

Hover and Vertical Climb Analysis

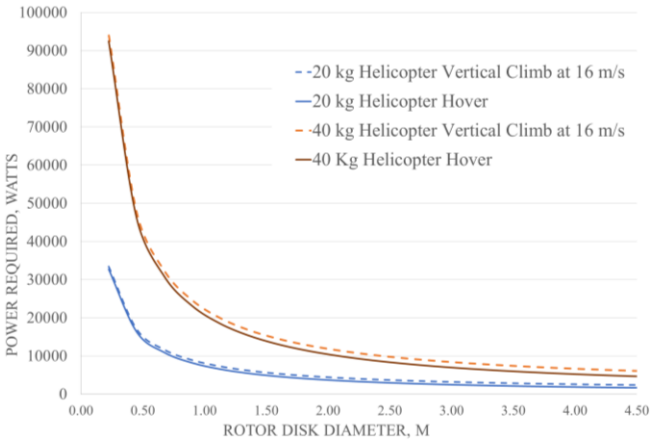

Fig. 3 Power Required vs Rotor Disk Diameter (Area) - 20 kg & 40 kg Martian Conventional Helicopter

We can observe in Fig. 3, a plot depicting the power required for a Martian helicopter of conventional scheme as a function of increasing rotor disk diameter. As the rotor diameter increases, the rotor disk area also expands, leading to a reduction in disk loading (represented as the total weight divided by the disk area, W/S). Essentially, lower disk loading means that less battery power is needed for hovering or climbing, which in turn allows for a higher power loading (W/P). However, it is important to note that lower disk loading corresponds to larger rotor blades, which contribute to increased weight, higher drag during forward flight, and a greater likelihood of encountering shocks on the advancing blade [16], which are not focused on in this research. The graph illustrates that smaller-sized rotors consume significantly more power than larger rotors, and there is a noticeable and dramatic decrease in power as the rotor disk diameter increases (also discussed in [22]). It is worth mentioning that, if the total mass of the aerobot is increased, the required power for smaller rotor disks becomes manifold high and the exponential decrement shifts towards the right and gradually stabilises. This disparity is illustrated in the 40 kg vs 20 kg Helicopter graph plot in Fig. 3. When examining the power requirements, it is evident that the helicopter's

power for vertical climbing is slightly higher than that for hovering, as expected due to the energy needed to generate vertical forward propulsion. However, as the rotor disk size increases, the difference between the two power requirements becomes more pronounced over time.

Fig. 4 and Fig. 5 illustrate graphical representations of hover power and vertical climb power (at a velocity of 60.61 m/s), respectively, in relation to the rotor disk diameter for various rotorcraft configurations. These configurations include the conventional helicopter, LS (large separation) coaxial rotorcraft, three tandem rotorcraft cases, and 2 isolated rotors rotorcrafts. The extension of the power data of 2 isolated rotors is for analytical comparison with tandem rotor Case 1, rather than for practical use. Similar to the trend observed in helicopter power requirements, all configurations exhibit higher power demands for vertical climbing compared to hovering, and the difference gradually increases with an increase in rotor disk diameter. Among these configurations, the conventional helicopter requires the most power. Comparatively, the power consumption of two equal-sized coaxial rotors is lower when using smaller-sized rotors, in contrast to the conventional helicopter. For example, at a rotor size of 0.23 m in diameter, the coaxial rotorcraft requires approximately 7,000 Watts less power, while all other configurations require about 12,000 Watts less power for both hovering and vertical ascent compared to the conventional helicopter. At the maximum aeroshell size, corresponding to a rotor diameter of 4.5 m, the power requirements for hover range between 1,000 to 2,000 Watts for all configurations. However, for vertical climbing, all configurations require less than 2,000 Watts except for the conventional setting, which demands significantly higher power than the others.

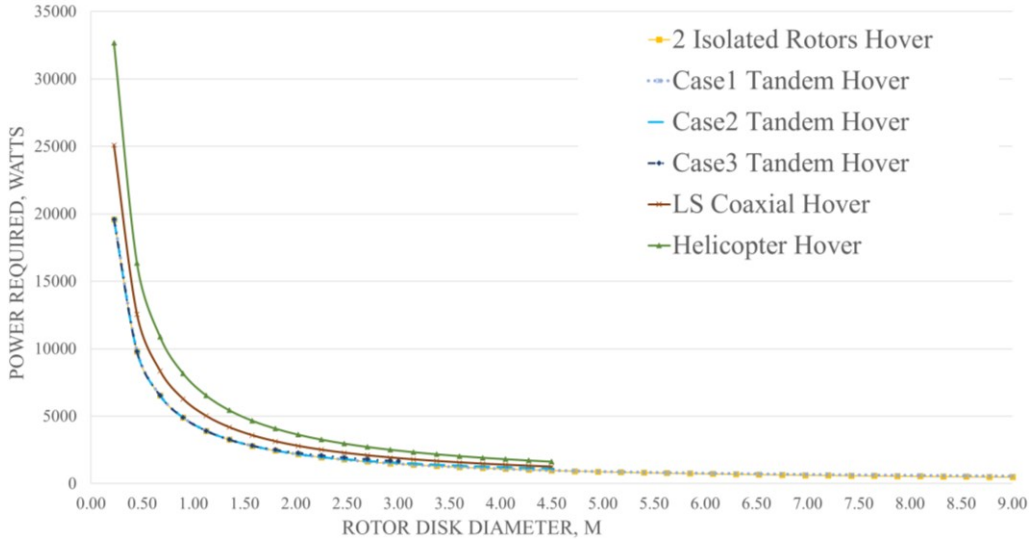

Fig. 4 Hover Power Required vs Rotor Disk Diameter (Area) – Comparison between various 20 kg rotorcraft configurations (2 Isolated Rotors, Tandem Cases, Coaxial, Helicopter)

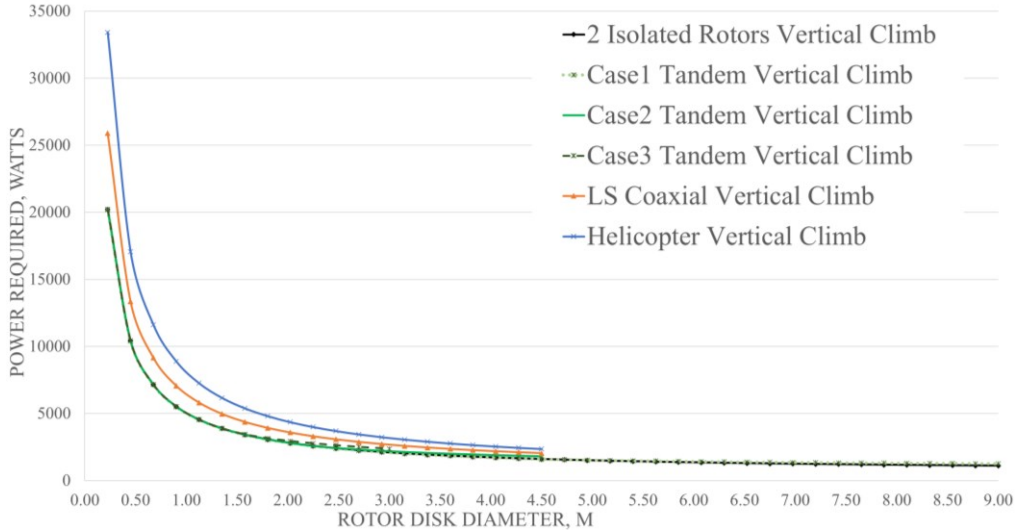

Fig. 5 Vertical Climb Power Required (at 16 m/s) vs Rotor Disk Diameter (Area) – Comparison between various 20 kg rotorcraft configurations (2 Isolated Rotors, Tandem Cases, Coaxial, Helicopter)

For the three tandem rotorcraft cases, it is noticeable that before any overlapping occurs between the rotors, the power required for the tandem rotorcraft system matches that of the two isolated rotors. In all configurations, the power requirements decrease exponentially and become relatively stable as the rotor diameter increases. This change becomes negligible, as seen in tandem rotorcraft Case 1, for rotor disk size values between 4.5 m and 9 m. Notably, tandem rotorcraft consumes considerably less power than all other rotorcraft configurations when using smaller rotor sizes.

Forward Flight Analysis

The forward levelled flight and forward climb flight at a 20-degree climb path angle are analysed for all the above-mentioned rotorcraft configurations at the forward flight speed of 60.61 m/s. Fig. 6 shows the required power for the forward flight of a Martian conventional helicopter against the increasing rotor disk size. Climbing up while flying forward requires higher power than the forward flight, and this phenomenon can be observed in the graph. However, at shorter rotor disk sizes the power consumption of both flights is similar to each other, and it is not until and beyond the rotor disk diameter of about 0.5 m that the difference between the two power requirements starts to become noticeable. The power requirements for forward climb flight do not decrease as much as the levelled flight, with the increasing rotor disk size. Fig. 7 depicts a snapshot of the power requirement of the forward levelled flight of all the selected configurations of rotorcrafts against the rotor disk sizes of up to 4.5 m. It can be noted that at the given smallest rotor disk size the conventional helicopter power has the highest and unrealistic power demand, followed by coaxial rotorcraft, tandem rotorcraft cases, and then 2 isolated rotors. Whereas, with the slight increase of rotor disk size, the power requirement drops down dramatically, until the change in the decrease in power becomes negligible from onward rotor size of 2 m.

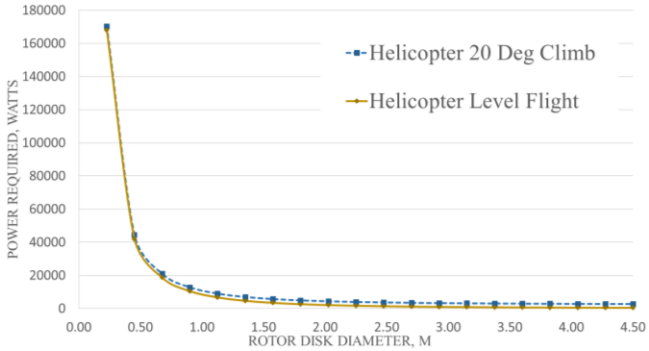

Fig. 6 Forward Flight Power Required (at 60.61 m/s) vs Rotor Disk Diameter (Area) - 20 kg Martian Conventional Helicopter

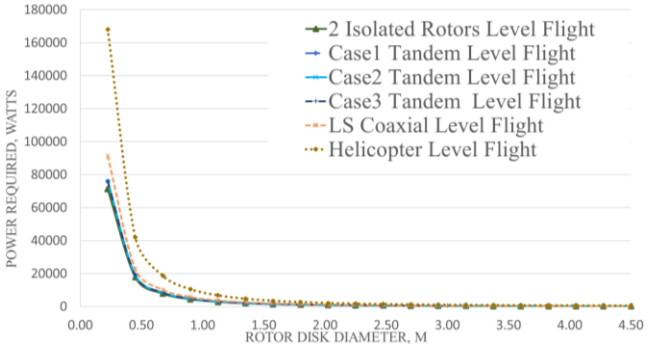

Fig. 7 Forward Level Flight Power Required (at 60.61 m/s) vs Rotor Disk Diameter (Area) - 20 kg Martian Various Rotorcraft Configurations

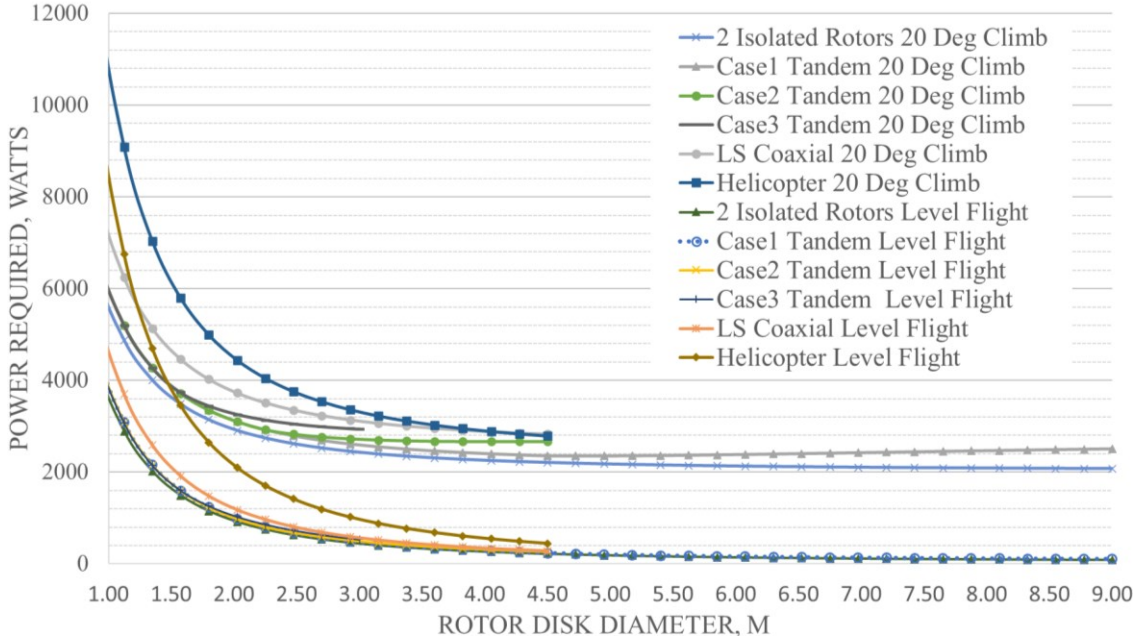

Fig. 8 Forward Flight Power Required (at 60.61 m/s) vs Rotor Disk Diameter (Area) – Comparison between various 20 kg rotorcraft configurations (2 Isolated Rotors, Tandem Cases, Coaxial, Helicopter)

Fig. 8 shows a close-up observation of the differences in required powers between these rotorcraft configurations for both forward levelled and climb flights, by setting off the rotor disk diameter from 1 m on the horizontal axis. An interesting behavior can be noticed with the forward climb of tandem rotorcraft Case 1, where the power required starts to increase after reaching a minimum value at a certain overlapping rotor disk size. This happens when the tandem rotors begin to overlap with each other, for case 1 it is beyond the rotor diameter of 4.5 m, because of the additional overlapping interference factor (K_{ov}) along the downwash factor (K_{dw}). The same trend is noticed with Case 2 tandem rotorcraft, but just at the upper limit of the rotor diameter.

It can be appreciated that forward levelled flight of all rotorcraft configurations starts to require under 1000 Watts of power for the rotor disk sizes beyond 3 m. Whereas, for forward flight at a climb angle of 20 degrees, the power requirement is about in between 2000 to 3000 Watts. Although climbing during a forward flight consumes higher power than the levelled flight, gaining height while flying forward is beneficial overall as it is more energy efficient than a plain vertical flight. Flying forward by staying closer to the ground creates air cushion under the aircraft that helps to gain the optimum flight speed before gaining altitude - a phenomenon called ground effects, which reduces energy losses. This analysis is performed at the maximum allowed forward flight speed to avoid the building up of air shocks at the rotor tip speed. However, if we experiment with increasing the forward speed further, the required power will decrease. Furthermore, the lower the climb path angle, the lesser the required forward climb flight power will be.

Efficient Rotor Configuration

A comparison of power requirements for hover and vertical climb between the LS coaxial rotorcraft and tandem rotorcraft Case 3 is presented in Fig. 9. The K_{ov} (overlapping interference factor) for LS (large separation) coaxial rotors is 1.281, whereas for tandem rotors Case 3, which allows for a maximum rotor diameter of 3 m (also where the maximum tandem rotors overlapping occurs), the K_{ov} is 1.134. Notably, the K_{ov} for Case 3 reduces as the rotor disk diameter diminishes below 3 m because of the reduction in rotors overlapping. An observable difference of approximately 1000 Watts can be noted for hover power at a rotor diameter of 1.5 m, where the tandem rotor has zero overlapping in this specific case. As a result, tandem rotor Case 3 appears to be a favorable configuration option, as it demonstrates higher hover and vertical climb power efficiency compared to the LS coaxial setting. Additionally, it is mechanically less complex due to the use of a rigid rotor hub system. For rotor disk sizes greater than 3 m, LS coaxial rotors could be considered, but the trade-off would be a higher K_{ov}. Alternatively, tandem rotor Cases 1 or 2 might be viable options, but they would require an articulated hub system with a folding mechanism, which adds complexity and weight to the overall system.

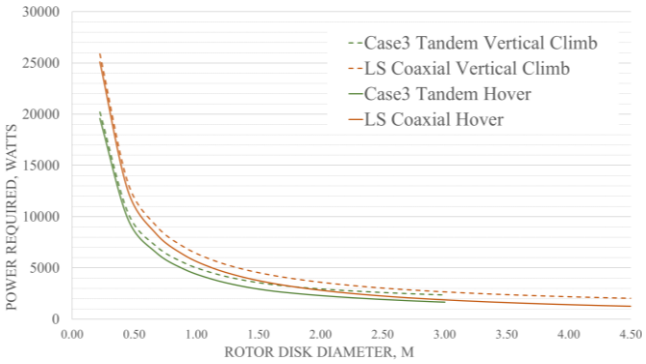

Fig. 9 Hover & Vertical Climb (at 16 m/s) Power Required vs Rotor Disk Diameter (Area) - 20 kg Case 3 of Tandem Rotorcraft and LS Coaxial Rotorcraft

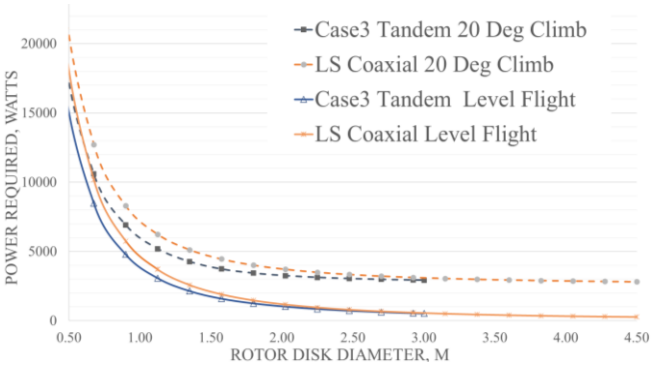

Fig. 10 Forward Flight Power Required (at 60.61 m/s) vs Rotor Disk Diameter (Area) - 20 kg Case 3 of Tandem Rotorcraft and LS Coaxial Rotorcraft

Similarly, Fig. 10 illustrates a comparison of these two cases for forward flight, it can be observed that there is not much difference between power requirements at the levelled flight. However, forward flight at a climb angle of 20 degrees has a greater difference at shorter rotor disk sizes, which gradually becomes smaller as the rotor disk sizes approach 3 m. Therefore, it is evident that tandem rotor Case 3 can be more efficient than its counterpart when flying at a climbing angle.

Comparative BMF Analysis of Different Rotor Configurations

In Fig. 11, a plot can be seen of the Battery Mass Fraction (BMF) calculated for the vertical climb required power for all the defined rotorcraft configurations, as it varies with increasing rotor disk diameter. This BMF is calculated considering a 1-minute run time (E), a climb speed of 16 m/s, and a fixed total mass of 20 kg. The trend of the vertical climb BMF lines mirrors the vertical climb power dependency shown in Fig. 5. Essentially, as the required power increases, the BMF also increases, which reflects the necessary battery weight for this specific flight segment. A similar BMF trend is observed for the forward levelled flight segments shown in Fig. 12, which reflects the power requirement of the forward levelled flight presented in Fig. 7.

Calculating the battery mass is simple; multiply the BMF by the total mass of the aircraft. For example, with a 0.02 BMF, the battery mass would equal 0.4 kg (i.e., 0.02 x 20 kg). It is important to note that the BMF of each segment must be aggregated with the BMF of other flight segments, as explained in section 3, to calculate the total BMF and determine the overall battery mass required for a particular flight regime. Additionally, it is worth mentioning that the BMF calculated for the flight mission does not include the battery mass needed for avionics or electronic payload instruments. These would require separate calculations unless these have dedicated batteries of their own.

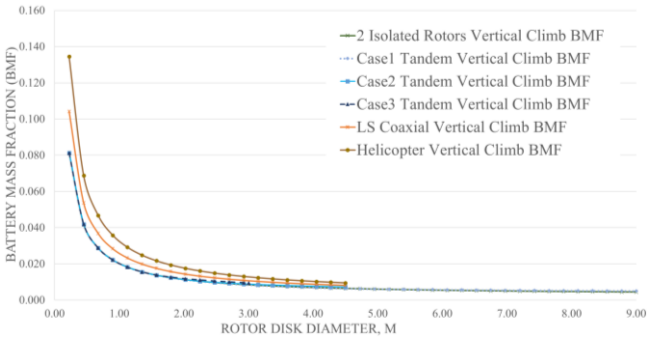

Fig. 11 Vertical Climb (at 16 m/s) BMF vs Rotor Disk Diameter (Area) - 20 kg Martian rotorcrafts

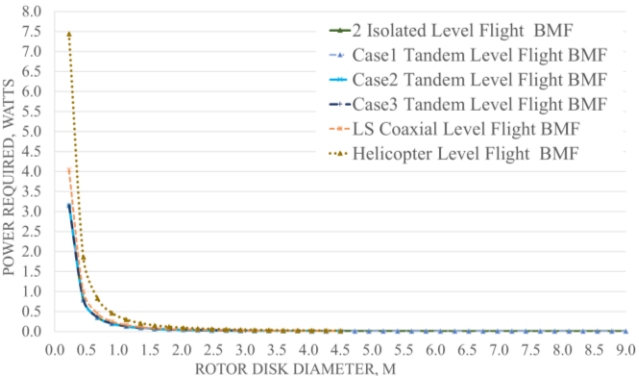

Fig. 12 Forward Levelled Flight (at 60.61 m/s) BMF vs Rotor Disk Diameter (Area) - 20 kg Martian rotorcrafts

6. Conclusion

The successful flight of the first Mars Helicopter has demonstrated the feasibility of rotorcraft flight on Mars. Building on this knowledge, future Mars rotorcraft will require advanced solutions. This paper addressed the research gap, outlined the mission statement, and defined fundamental parameters for conducting a parametric study of various 20 kg rotorcraft with single and dual rotor configurations. The methodology employed is based on simplified helicopter momentum theory equations, which are elucidated for each rotorcraft configuration and further refined with estimations. Additionally, the paper introduces a methodology for the initial sizing of battery-electric aircraft, including the calculation of Battery Mass Fraction for flight segments to determine the necessary battery mass. A graphical representation illustrating the power required for hover, vertical climb, and forward flight as a function of increasing rotor disk diameter is presented for several rotorcraft types, including conventional helicopters, coaxial rotorcraft, tandem rotorcraft, and rotorcraft with two isolated rotors. Notably, the conventional helicopter at the given parameters consumes more power than all other configurations within the set parameters. Rotorcraft with two isolated rotors is considered an ideal configuration as they do not overlap, and thus do not experience overlapping aerodynamic interference. Among tandem rotor configurations, tandem rotor Case 3 demonstrates overall efficiency, particularly for rotor disk sizes up to 3 m, when compared to other configurations. It is worth mentioning that as rotor disk diameter approaches the upper limit of the allowed disk size, the differences in power requirements between all configurations become negligible at a macro level.

7. Future Work

Based on our comprehensive analysis and the resulting data, we have derived power consumption estimates for a range of Martian rotorcraft configurations, specifically focusing on hover, vertical climb, and forward flight phases. Our ongoing research activities now encompass an in-depth investigation into the power consumption associated with rotorcraft's overall flight envelope, both in configurations with and without wings. Our objective is to provide a comprehensive and conclusive assessment that thoroughly outlines the advantages and disadvantages inherent in different rotorcraft configurations. We aim to deliver a formal and informative research package that can be of substantial utility to Martian aerobot designers. By furnishing them with theoretical estimates and valuable performance insights, our research endeavors to empower designers in the thoughtful selection of the most optimised rotorcraft configuration, aligning it precisely with the distinct requirements of their mission.

References

[1] Hassanalian, M., Rice, D., & Abdelkefi, A. Evolution of space drones for planetary exploration: A review. Progress in Aerospace Sciences, 97, 2018. 61–105. https://doi.org/10.1016/J.PAEROSCI.2018.01.003

[2] NASA. Overview | Mars – NASA Solar System Exploration. Retrieved November 25, 2023, from https://solarsystem.nasa.gov/planets/mars/overview/

[3] Radotich, M., Withrow-Maser, S., deSouza, Z., Gelhar, S., & Gallagher, H. (2021, January). A study of past, present, and future Mars rotorcraft. In 9th Biennial Autonomous VTOL Technical Meeting.

[4] Johnson, W., Withrow-Maser, S., Young, L., Malpica, C., Koning, W. J. F., Kuang, W., Fehler, M., Tuano, A., Chan, A., Datta, A., Chi, C., Lumba, R., Escobar, D., Balaram, J., Tzanetos, T., & Fjaer Grip, H. (2020). Mars Science Helicopter Conceptual Design. http://www.sti.nasa.gov

[5] NASA. Mars Helicopter - NASA Mars. Retrieved January 05, 2024, from https://mars.nasa.gov/technology/helicopter/#Flight-Log
[6] Young, L. A., Chen, R. T. N., Aiken, E. W., Briggs, G. A., "Design Opportunities and Challenges in the Development of Vertical Lift Planetary Aerial Vehicles," Proceedings of the American Helicopter Society International Vertical Lift Aircraft Design Specialist's Meeting, January 2000.
[7] Aguirre, J., Casado, V., Chamie, N., & Zha, G. (2007). Mars Intelligent Reconnaissance Aerial and Ground Explorer (MIRAGE) AIAA 2007-244. https://doi.org/10.2514/6.2007-244
[8] Forshaw, J., & Lappas, V. (2012). Architecture and Systems Design of a Reusable Martian Twin Rotor Tailsitter. Acta Astronautica, 80(0), 166–180. https://doi.org/10.1016/J.ACTAASTRO.2012.05.008
[9] RM Zubrin. (2012). The Mars Gashopper - Concepts and Approaches for Mars 2012. https://ui.adsabs.harvard.edu/abs/2012LPICo1679.4069Z/abstract
[10] NASA. NASA TechPort - Project Data. Retrieved November 25, 2023, from https://techport.nasa.gov/view/93850
[11] Boelhouwer, R.N.J., Bunschoten, E.C., Debusscher, C.M.J., Frijters, W., van Goeverden, R.J., Legrand, E.B., Matton, J., Paliusis, K., and Verheyen, J.K.N. "Design Report, Martian Advanced Reconnaissance System." Delft University of Technology, June 2018.
[12] Underwood, C., & Collins, N. (2017). Design and Control of a Y-4 Tilt-Rotor VTOL Aerobot for Flight on Mars. Proceedings of the 68th International Astronautical Congress (IAC), 25–29. https://openresearch.surrey.ac.uk/esploro/outputs/conferencePresentation/Design-and-Control-of-a-Y-4-Tilt-Rotor-VTOL-Aerobot-for-Flight-on-Mars/99511131102346
[13] Denys, K. Ukrainian invention to feel the ground for Mars colonization (GRAPHICS) - Jun. 06, 2016 | KyivPost. Retrieved November 25, 2023, from https://www.kyivpost.com/article/content/ukraines-it-edge/ukrainian-invention-to-feel-the-ground-for-mars-colonization-graphics-415570.html
[14] Fathepure, M., Booker, A. L., Abouzahr, O., Wang, N., & Tikalsy, D. (2021). Design and Construction of an Inflatable-Winged VTOL Mars Electric Flyer. In AIAA AVIATION 2021 FORUM (p. 2578) https://doi.org/10.2514/6.2021-2578
[15] S. Withrow, W. Johnson, L. A. Young, H. Cummings, J. Balaram, and T. Tzanetos, "An Advanced Mars Helicopter Design," in ASCEND 2020, American Institute of Aeronautics and Astronautics.
[16] D. Raymer. Aircraft design: A conceptual approach, 6. Ed., AIAA education series, Reston, Va., 2018, Chaps. 20.11, 21.3.
[17] Leishman, J. Gordon. Principles of Helicopter Aerodynamics, 2. Ed., United Kingdom, Cambridge University Press, 2006. Chaps. 2.15, 5.5.11.
[18] Johnson, W. Rotorcraft Aeromechanics. Cambridge University Press. 2013. Chaps. 4.6, 5.3. https://doi.org/10.1017/CBO9781139235655
[19] NASA. Mars Fact Sheet. Retrieved November 03, 2023, from https://nssdc.gsfc.nasa.gov/planetary/factsheet/marsfact.html
[20] Millour, E., Forget, F., Spiga, A., Pierron, T., Bierjon, A., Montabone, L., Vals, M., Lefèvre, F., Chaufray, J.-Y., Lopez-Valverde, M., Gonzalez-Galindo, F., Lewis, S., Read, P., Desjean, M.-C., and Cipriani, F. and the MCD Team: The Mars Climate Database (Version 6.1), Europlanet Science Congress 2022, Granada, Spain, 18–23 Sep 2022, EPSC2022-786, https://doi.org/10.5194/epsc2022-786
[21] Balaram, J., Aung, M., & Golombek, M. P. (2021). The Ingenuity helicopter on the Perseverance rover. Space Science Reviews, 217(4), 56. https://doi.org/10.1007/s11214-021-00815-w
[22] Youhanna V, Felicetti L & Ignatyev D (2023) Parametric analysis of battery-electric rotorcraft configurations to fly on Mars. In: Aerospace Europe Conference Joint 10th EUCASS - 9th CEAS Conference 2023, Lausanne, 9-13 July 2023. DOI: 10.13009/EUCASS2023-319

BIOGRAPHY

Vishal Youhanna *is a PhD researcher at Cranfield University, UK. His project is to design a rotorcraft for flying on Mars. He completed his BEng Hons Degree in Aerospace Engineering from the University of Hertfordshire, UK in 2016. During his degree, he worked at Pall Corporation UK as a Research and Development Engineer Undergrad for a year. After graduating he temporarily moved to Australia, where he studied business and management, along with directing and managing a small technology business. His passion for aerospace and research brought him back to the UK in 2021 to pursue a PhD in Aerospace.*

Leonard Felicetti *is a Senior Lecturer in Space Robotics and Guidance Navigation and Control at Cranfield University (UK). He obtained his Ph.D. and he was a Post-Doc Researcher in Sapienza - University of Rome (Italy). In 2015, he was an Honorary Research Associate at the University of Glasgow (UK), and then, Associate Senior Lecturer in On-board Space Systems at Luleå University of Technology (Sweden). He joined Cranfield University (UK) in 2019, he currently leads both the teaching and research activities in Guidance, Navigation and Control of Space Systems, Spacecraft Orbital and Attitude Control Systems, and Space Robotics.*

Dmitry Ignatyev *is a Senior Research Fellow in the Autonomous Systems and Control Centre for Autonomous and Cyberphysical Systems at Cranfield University, UK. He received a PhD in Physics and Mathematics from the Moscow Institute of Physics and Technology (MIPT) in 2013. Before joining Cranfield, Dr Ignatyev worked for eight years as a researcher at the Central Aerohydrodynamic Institute n.a. Zhukovsky, a leading aeronautics research institution in Russia. He is actively involved in teaching activities of the centre and is currently a leader of the "Modelling and Simulation" module within the Autonomous Vehicles Dynamics and Control course. He has published over 30 journal and conference papers on aerodynamics, flight dynamics, and control.*

2024-05-13

Conceptual design study based on defined parameters for next-generation Martian rotorcrafts

Youhanna, Vishal

IEEE

Youhanna V, Felicetti L, Ignatyev D. (2024) Conceptual design study based on defined parameters for next-generation Martian rotorcrafts. In: IEEE Aerospace Conference, 02-09 March 2024, Big Sky, MT, USA

https://doi.org/10.1109/AERO58975.2024.10521441